Informational Memory Shapes Collective Behavior in Intelligent Swarms

Shengkai Li,[1,*,†] Trung V. Phan,[2,*] Luca Di Carlo,[1] Gao Wang,[3] Van H. Do,[4]
Elia Mikhail,[5] Robert H. Austin,[1,‡] and Liyu Liu[6,§]

[1]*Department of Physics, Princeton University, Princeton, New Jersey 08544, USA*
[2]*Department of Natural Sciences, Scripps and Pitzer Colleges, Claremont Colleges Consortium, Claremont, California 92110, USA*
[3]*Wenzhou Institute, University of Chinese Academy of Sciences, Wenzhou, Zhejiang 325000, China*
[4]*Department of Physics, University of Massachusetts, Boston, Massachusetts 02125, USA*
[5]*Department of Electrical and Computer Engineering, Princeton University, Princeton, New Jersey 08544, USA*
[6]*Human Phenome Institute, Fudan University, Shanghai 201203, China*

(Received 3 July 2025; revised 12 November 2025; accepted 3 March 2026; published 31 March 2026)

We present an experimental and theoretical study of 2-D swarms in which collective behavior emerges from both direct local mechanical coupling between agents and from the exchange and processing of information between agents. Each agent, an air-table drone endowed with internal memory and a binary decision variable, updates its state by integrating a time series of memories of local past collisions. This internal computation transforms the swarm into a dynamical information network in which history-dependent feedback drives spontaneous complete spin polarization, pitchfork bifurcated spin collectives, and chaotic switching between collective states. By tuning the depth of memory and the decision algorithm, we uncover a memory-induced phase transition that breaks spin symmetry at the population level. A minimal theoretical model maps these dynamics onto an effective potential landscape sculpted by informational feedback, revealing how temporally correlated computation can replace instantaneous forces as the driver of collective organization, informed by experiments. These results position physically interacting drone swarms as a model system for exploring the physics of informational drone ensembles whose emergent behavior arises from the interplay between physical interaction and information processing.

DOI: 10.1103/rt97-ncmf

Introduction—Many living systems exhibit behaviors shaped by past interactions, with memory depth playing a crucial role. Birds align with neighbors to form flocks [1], bacteria integrate chemical signals to navigate [2,3], and humans vote or invest based on memories [4]. Such responses extend beyond immediate stimuli and involve information processing. Memory-based feedback can generate complex behaviors, such as nonreciprocal interactions [5]. Memory-influenced opinion dynamics exemplifies this and has attracted sustained interest [6–11] [Fig. 1(a)], with political polarization shaped by how people recall and evaluate past events [12].

Here we work with agents that autonomously control their rotation and update a binary spin state interpreted as opinion [15–18]. Agents perceive the spin of colliding partners and modify their own spin based on memory and decision rules, reflecting "personalities" such as conformity, contrarianism, or stubbornness [19] [Fig. 1(a)]. Although physical collisions follow deterministic laws [13], agent responses are driven by informational feedback. Personality remains fixed [Fig. 1(b)], but memory processing enables spontaneous polarization, oscillations, and chaotic transitions at the collective level [20–22]. Although memory was introduced to improve single-agent spin-detection reliability, its impact on population dynamics reveals a broader principle. Instead of suppressing fluctuations through enhanced sensing accuracy or stronger inter-agent coupling, strategies that may be costly or impractical, we pursue an alternative route based on agents' memory of and action on past events. Because memory is readily implemented in robotic systems, it provides a minimal mechanism to average out noise and drive unexpected collective dynamics.

This system exemplifies how sensing, actuation, and memory generate adaptive collective behavior [23]. Unlike many active matter studies with fixed chirality, our agents use memory-based interactions linking past encounters to macroscopic order, offering an interpretable model of informational feedback. The results advance nonreciprocal dynamics [5,17,24], complement social-polarization models [6,7], and extend chiral-ensemble studies [25–28] to systems whose spins are set by internal states. Earlier work

[*]These authors contributed equally to this work.
[†]Contact author: shengkaili@princeton.edu
[‡]Contact author: austin@princeton.edu
[§]Contact author: liuliyu@fudan.edu.cn

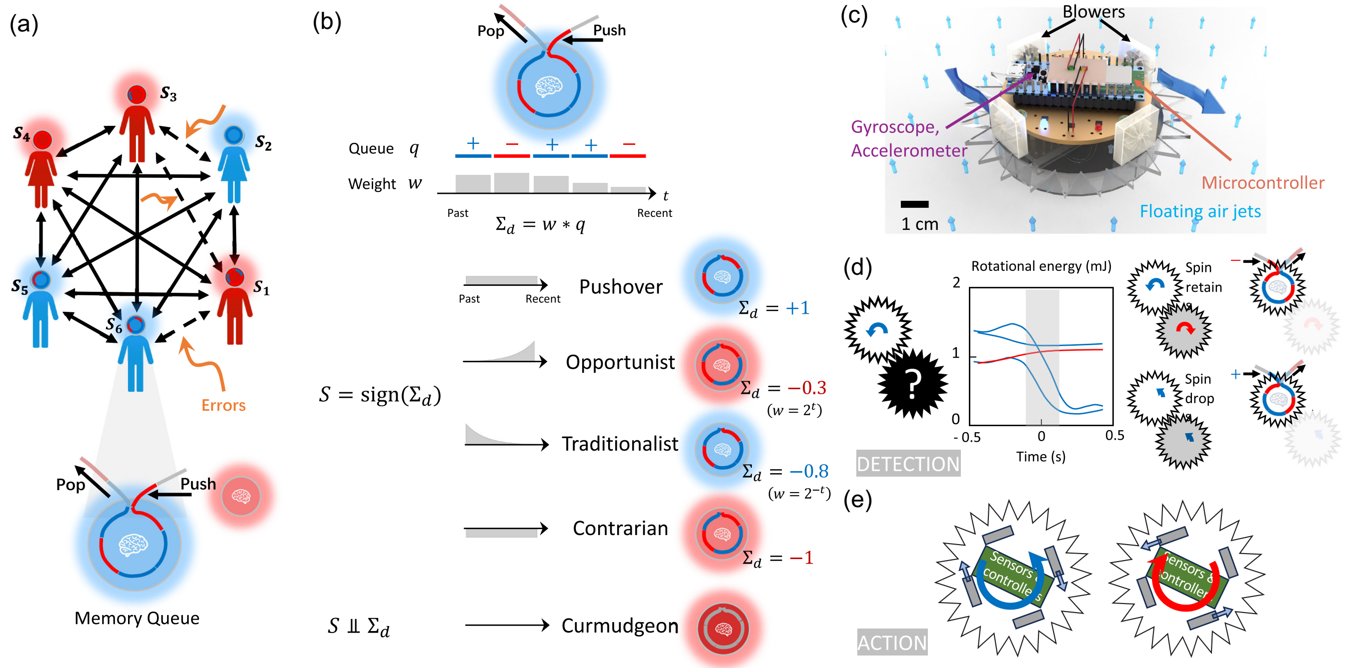

FIG. 1. Opinion exchange. (a) Individuals update their opinions by evaluating others' states using a finite memory of recent observations stored in a queue. (b) The state updates with weighted memory $\Sigma_d = \sum_i w_i q_i$. Observations $q_i \in \{+1, -1\}$ are weighted by w_i depending on their personalities. A pushover follows the majority where w_i is constant such that $S = \mathrm{sign}(\Sigma_d)$ picks the spin with larger counts. Negative constant weight defines an agent against the majority, and higher weights on the more recent events defines an opportunist. Curmudgeons with strong biases have independence of weighted memory. (c) A physical agent (spinner) has a microcomputer with gyroscope, accelerometer, and actuates the state with four blowers. (d) A spinner records information of surrounding spinners through mechanical interactions (gray shades) that same spins drop spin upon collision while opposite spins do not [13]. (e) A spinner chooses its spin direction by selecting appropriate blowers depending on its internal algorithm. See SI1.mp4 in [14] for demonstration.

on memory in collective dynamics includes opinion-formation models that integrate all past neighbors [29], robotic active matter with passive sensorial delay [30], and hydrodynamic feedback yielding emergent chirality reversal [31]. Here, each agent retains a tunable, finite record of recent interactions, allowing controlled responsiveness and stability. This finite, programmable memory is an internal degree of freedom governing symmetry breaking and collective organization.

Embedding computation, memory, personality, and communication—The drones are driven spinning gears floating on an air table, with an Arduino microcomputer, sensors, and blowers to direct tangential air flow. Among the sensors, the accelerometer detects collision events while the gyroscope determines spin changes. Depending on the information the microcomputer gets from the sensors and the history of previous collisions and how it interprets past events, each spinner makes a decision to possibly alter its intrinsic spin by actuating the blowers to change their spin see (Fig. 1).

The ability to recognize another agent's spin direction arises from physics of collisions between spinning and translating bodies [13], akin to antiferromagnetism [32]: collisions between same-handed spinners reduce both spins, while opposite-handed ones retain their spins. Each spinner has four blowers arranged so that activating one pair produces counterclockwise (+) motion and the other clockwise (−).

When a collision is detected via the accelerometer and the colliding agent's spin is inferred from the gyroscope, the result is pushed onto an M-bit queue. Due to complex collision dynamics, spin determination is imperfect; the current setup achieves 70% accuracy. Thus, the stored sequence of $+1$'s and -1's, representing past collisions, is not exact.

The memory depth M is set before each experiment, ranging from 1 (only the previous collision stored) to 21. The queue operates first-in, first-out. The spinner sets its spin based on the weighted sum of the queue $\Sigma_d = \sum_{i=1}^{M} w_i q_i$, where q_i is the i th spin and w_i its weight. This convolution of memory and kernel resembles how bacteria assess chemoattractant gradients over time [2,3]. As bacteria choose to run or tumble, our spinner chooses spin direction via $s = \mathrm{sign}(\Sigma_d)$, a nonlinear feedback that may enhance polarization [33].

For example, a pushover spinner sets all weights $w_i = 1$ and aligns its spin with the sum of past M events, seeking consensus. A curmudgeon remains fixed at $+$ or $-$ regardless of events. An opportunist favors recent events,

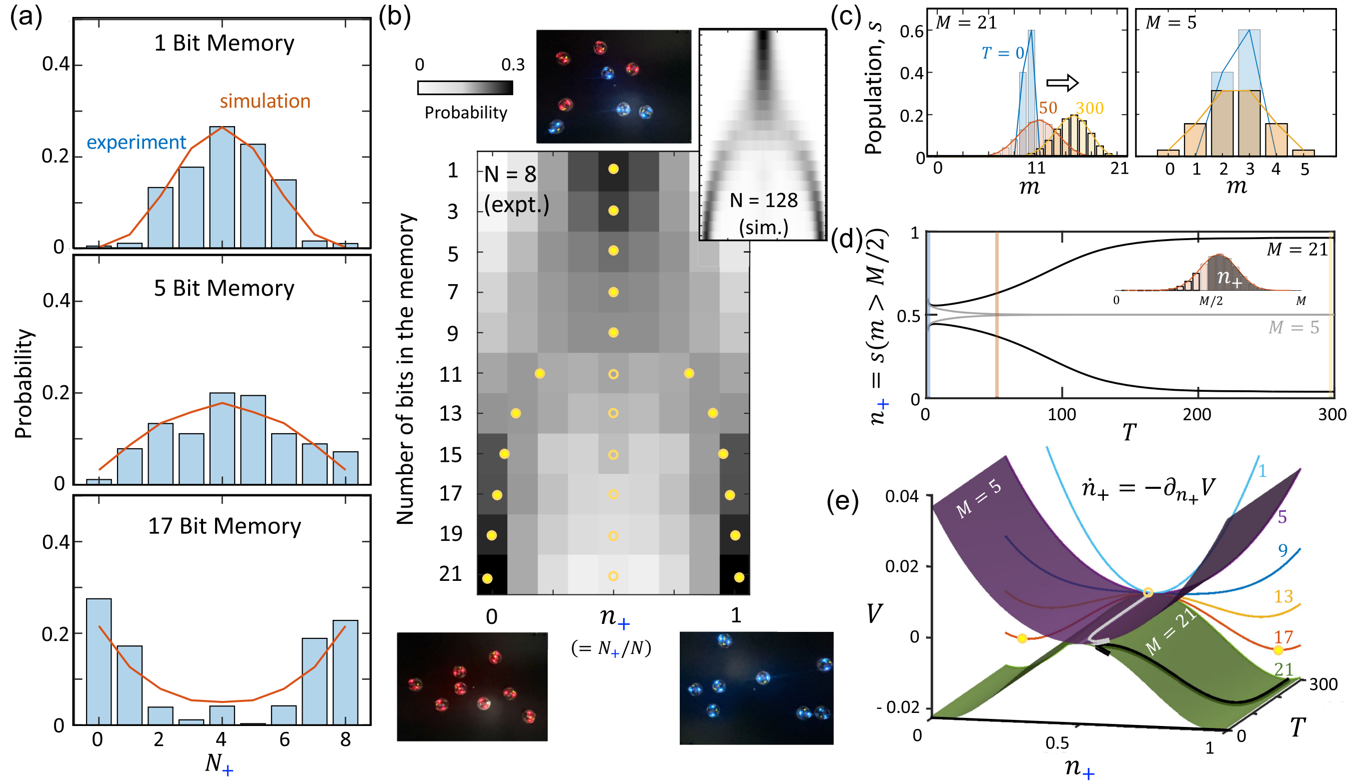

FIG. 2. Memory-induced spontaneous symmetry breaking. (a) Probability of states for a collective of pushover with each building its memory of past M collision inference and following the majority in memory for different M. (b) Experiments (SI2.mp4 in [14]) show that polarization is absent at small M and emerges at large M. The inset shows simulation (SI7.mp4 in [14]) results for large N$(=128)$. (c) Population over time for spinners with m bits of +. When the initial population of + spinners is slightly higher than − spinners, memory size $M = 21$ attracts the population to higher + memory states while $M = 5$ erases the initial bias and leads the collective to an even distribution of + and −. (d) The fraction of + over time for $M = 5$ and $M = 21$ with detection error $\eta = 0.3$. (e) The fraction of + spinners $n_+ = N_+/N$ follows the gradient of an effective potential V which varies from a single well when M is small to a double well when M exceeds a critical value.

while a traditionalist emphasizes the most distant ones. A contrarian sets its spin opposite to the majority in its memory.

Although each spinner's state is binary (+ or −), its detailed memory affects its response to collisions. For instance, a 5-bit + pushover with $(3+, 2-)$ is more likely to change than one with $(5+, 0-)$ (a deep + state). We later show how the evolution of these finer substates influences emergent consensus. Our agents decide future spin based on past experiences, enabling highly non-Markovian behavior, diverging from purely physics-based systems. For example, pushovers align with the perceived majority spin, even if sampled with error, resembling human information processing [34,35].

Memory-induced spontaneous symmetry breaking of pushovers—Starting with equal numbers of + and − spinners, spontaneous symmetry breaking can occur due to nonlinear interactions [36], depending on decision rules, noise, and especially memory depth M. When $M = 1$, the collective stays around 50/50 (Fig. 2). But for larger memory, e.g., $M = 17$, initially unpolarized spinners settle into either all + or all − states, each with 50% probability set by initial conditions, indicating spontaneous symmetry breaking. A sharp transition from no polarization to symmetry breaking occurs around $M \sim 9$ (Fig. 2), resembling tipping points in complex systems like ecological transitions with early warnings [37].

To build an intuition for spontaneous symmetry breaking, we studied how populations with different memory configurations evolve. The current population of spinners with m bits of + in memory, s_m where $0 \leq m \leq M$, is contributed by three populations in the past: (1) spinners that had m bits of + and did not change their state, (2) spinners that had $m - 1$ bits of + and then detected another + spinner, (3) spinners that had $m + 1$ bits of + and detected another − spinner.

As an example, we apply the above to a collective with an initial population of + spinners slightly higher than − spinners. With memory size $M = 21$, the population is attracted to higher + memory states. In contrast, when $M = 5$, the population evolution erases initial bias and leads the collective to an even distribution of + and −

[Figs. 2(c) and 2(d)]. By tracking the transition of memory configurations (strings of $+/-$) (Sec. I.A in [14]), we can show that the fraction of $+$ spinners, $n_+ = N_+/N$ where N_+ and N are the numbers of $+$ spinners and total spinners, follows the gradient of an effective potential well V with $\dot{n}_+ = -(1/\tau)[\partial V/\partial n_+]$, where τ is the average state updating time. The memory size M and detection error η shape the potential well as

$$V = \frac{1}{2}\left[1 - (1-2\eta)\sqrt{\frac{2M}{\pi}}\right]\left(n_+ - \frac{1}{2}\right)^2 + O(n_+^4), \quad (1)$$

where the $O(n_+^4)$ expansion is $[(1-2\eta)^3/3\sqrt{2\pi}]\,M^{3/2}(n_+ - 0.5)^4$.

As memory size M increases, the quadratic term changes sign, the potential becomes double welled, and a supercritical pitchfork bifurcation occurs [38]. Lower detection error η also promotes this transition. The critical memory $M_c = \pi/2(1-2\eta)^2$ yields 9.8 bits for the 30% error rate observed experimentally, matching the transition point. A scan of symmetry breaking, via variance $\sum_i (n_{+,i} - 0.5)^2 p_i$, confirms this criticality (Sec. I.A in [14]). The memory-error dependence resembles polarization in opinion-dynamics models [12]. Unlike Axelrod's agents, which form simultaneous opposing clusters, our spinners occupy one extreme at a time and collectively switch. Simulations with larger $N = 128$ confirm a bifurcation near $M = 10$ (Fig. 2).

The above demonstrates non-Markovian effects in systems with evolving internal states [39,40]. In Markovian limit $M = 1$, reciprocal interactions yield equipartition of microstates and binomial distributions for N_+ (Sec. I.B in [14]). Larger M strengthens non-Markovianity, producing qualitatively different collective behavior beyond timescale effect. Symmetry breaking persists under error, and tolerance rises with memory depth.

Polarization can also be viewed as a limit of reliable information transmission [41,42]. Each collision transmits one noisy bit about the collective state through a binary symmetric channel with error η and Shannon capacity $C = 1 - H(\eta)$, where entropy $H(\eta) = -\eta\log_2\eta - (1-\eta)\log_2(1-\eta)$. An agent with memory depth M acts as a length-M repetition encoder with majority decoding, giving rate $R = 1/M$. Shannon's theorem requires $R < C$, yielding $M_c \simeq 1/[1 - H(\eta)]$. For $\eta = 0.3$, this predicts $M_c \approx 8.4$, close to the observed transition near 9. Expanding $H(\eta)$ near $\eta = 0.5$ gives the same scaling $M_c \propto (0.5 - \eta)^{-2}$ as the state-transition theory, showing that symmetry breaking occurs when information transmission saturates channel capacity.

A curmudgeon among the pushovers—A curmudgeon follows its own fixed opinion [43] and responds nonreciprocally [5], unlike pushovers that react based on memory. Using Bluetooth, we changed curmudgeons' chirality to demonstrate their influence on pushovers

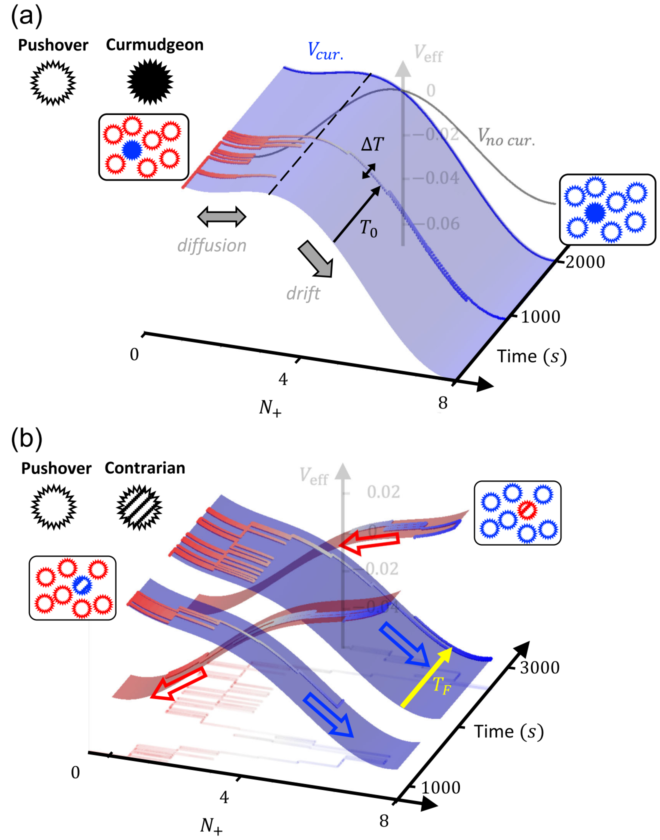

FIG. 3. Curmudgeon and contrarian. (a) Among pushovers with 27-bit memories (above critical), a curmudgeon has a constant opinion which is able to distort the symmetric double-well potential ($V_{\text{no cur.}}$) to a biased double-well ($V_{\text{cur.}}$). An experiment (SI3.mp4 in [14]) where a group of pushovers with all −bits get directed by a + curmudgeon after initial diffusion stage. (b) A contrarian opposing the majority behaves like a short-term curmudgeon (SI4.mp4 in [14]). Here $M = 17$.

(SI3.mp4 and Fig. S7 in [14]). Curmudgeons tilt the double-well potential [Eq. (1)]: even 12.5% (one of eighty spinners) significantly biases the system when $M = 27$ [Fig. 3(a), Sec. I.C in [14]]. Starting from all spinners in $-$ state, a single $+$ curmudgeon seeds a field-biased, nucleationlike switch to $+$. Unlike spontaneous classical nucleation [44], here the curmudgeon acts as a nucleation source. With both $+$ and $-$ curmudgeons present, the larger subpopulation typically wins; for equal numbers, the system undergoes a pitchfork bifurcation at a higher critical memory (Sec. IV.D in [14]). If curmudgeons randomly flip sign, they act as dissenters in a modified Vicsek model and raise the consensus threshold (Sec. IV.E in [14]).

Interestingly, when memory is below critical threshold ($M < M_c$), pushovers are not affected by curmudgeons and remain near a 50/50 split. To influence others, a curmudgeon needs a crowd that highly values peer opinions. At very large M, the crowd's shift toward the curmudgeon's state happens abruptly [20], due to slow diffusion across the barrier followed by rapid descent along a steep potential

[Fig. 3(a)]. This timescale gap widens with M, as diffusion time T_0 grows with memory size: $M^2 = \langle m(T_0)^2 \rangle \propto T_0$.

A contrarian among the pushovers—A contrarian sets its spin opposite the majority in its memory [45], often standing alone like a curmudgeon. As the crowd shifts toward it, new interactions reveal the change and it flips again, sustaining opposition. Experiments [Fig. 3(b)] show small phase delays from detection-response time to demographic changes.

The flipping interval T_F varies, with short T_F more common than long ones. Long T_F follows an exponential distribution, while short T_F approximates a power law (Fig. S8 in [14]), reflecting the time for a contrarian to overwrite its memory ($\sim M$ collisions). This drives the alternation between consensus states. It is more pronounced with high memory (Fig. S10 in [14]), which enhances attraction to each consensus well and accelerates transitions, as seen in curmudgeon experiments.

A minimal model coupling the contrarian and pushovers captures key dynamics. Pushovers influence the contrarian's memory: $\dot{c} = k_c p + \xi_c$, where p is the excess $+$ population and c the excess $+$bits in the contrarian. The contrarian, in turn, drives the population: $\dot{p} = -k_p \mathrm{sgn}(c) + \xi_p$. Coupling these gives

$$\ddot{c} = -k\mathrm{sgn}(c) + \xi, \tag{2}$$

where $\xi = \xi_p/k_p + \xi_c/k_p k_c$ and $k = k_c k_p$. This interaction produces consensus switching analogous to stick-slip dynamics. Large memory M causes sharp transitions, whereas intermediate "confused" states yield rapid flips. The flipping interval follows a power law (exponent ≈ -1.5) for short times, with an exponential tail scaling as M^2 [46]. Large M allows rare, long intervals that sustain demographic switching (Sec. I.D in [14]).

Contrarian-driven oscillations resemble the swap phase in nonreciprocal systems [47]. In our model, the memory depth M controls this behavior: small M generates a more homogeneous state while larger M produces the swap phase. This highlights memory depth as a key control of memory-bearing agents.

The traditionalist, pushover, and opportunist—Humans weigh past and recent memories differently [48–50]. We explore how exponential memory weight, $w \propto b^t$, influences opinion polarization. For $b = 1$, spinners are pushovers; $b > 1$ emphasizes recent events (opportunists); $b < 1$ favors distant ones (traditionalists). The same memory can make opposite decisions depending on the weight [Fig. 1(b)]. Starting all spinners with $-$ spin and $-$bits, we measure the time to reach an even distribution [Figs. 4(b) and 4(c)]. We find (1) traditionalists respond more slowly than opportunists; (2) response time grows with memory M and rises sharply at M_c, consistent with earlier results; (3) the peak occurs at $b = 1$ (pushover); (4) the above holds for larger N (Sec. IV.F in [14]).

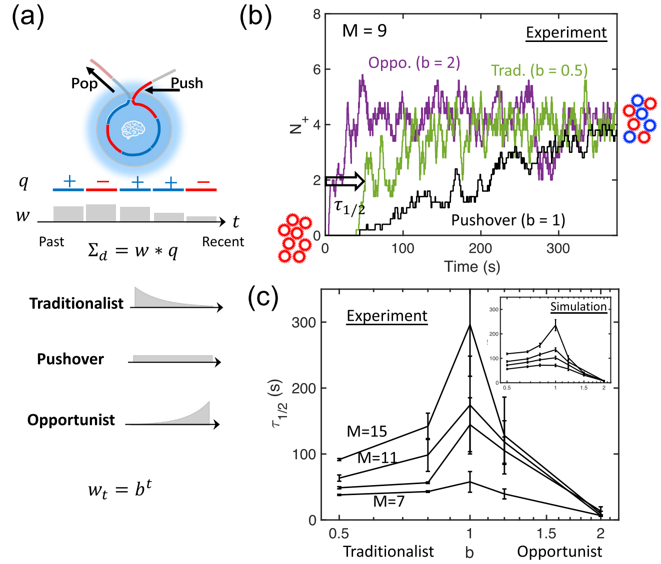

FIG. 4. Weighted memory. (a) The memory weight $w \propto b^t$ shifts its focus from the past to recent as weight bias b increases from 0. (b) The number of $+$ spinner, N_+, increases with time after all spinners start with pure $-$bits (SI5.mp4 in [14]). The growth rate varies among traditionalist, pushover, and opportunist. (c) Half-lives to reach 50/50 for different bias (b) and memory size (M).

Intuitively, opportunists' discount for older memory shortens effective memory and weakens symmetry breaking. Although weighting distant events seems to enhance the breaking, experiments and simulations show the opposite because outdated information dominates. In the limit $b \ll 1$, traditionalists rely on a single bit from M collisions earlier, behaving as originalists [51].

Conclusion—Our system is an ensemble where sensing, memory, and complex response generate adaptive collective behavior [23]. Unlike active matter driven by instantaneous forces or fixed design, agents here self-organize through information-driven dynamics that couple interaction history to motion, producing effective nonreciprocal interactions [5,17,24].

Using tools from statistical physics, we map collective opinion dynamics to a potential landscape, yielding a quantitative framework for memory-driven symmetry breaking. This extends chiral collective dynamics [25–28] to systems where handedness and coordination are emergent computational states, and complements social-polarization models [6,7]. Our results identify memory as a physical degree of freedom in nonequilibrium systems where past interactions shape future behavior and enable studies of memory-driven collectives that sense, learn, and react [52,53].

Acknowledgments—The authors acknowledge the very helpful and valuable advice from the referees. We thank Stanley H. Chidzik for PCB manufacture, Huaicheng Chen for tracking codes, Michael te Vrugt for valuable discussions at the early stage of this research; Robert Axelrod, Jie Bao, Ruihua Fan, Daniel Goldman, Stanley Nicholson, Miloš Nikolić, Huy D. Tran, and Bryan VanSaders for helpful discussions; and Jakob Möllmann for correcting typos and errors. This work was supported by the Center for the Physics of Biological Function at Princeton University and the National Natural Science Foundation of China (Grants No. T2350007, No. 12404239, and No. 12174041).

Data availability—The data that support the findings of this article are openly available [54], embargo periods may apply.

[1] T. Vicsek, A. Czirók, E. Ben-Jacob, I. Cohen, and O. Shochet, Novel type of phase transition in a system of self-driven particles, Phys. Rev. Lett. **75**, 1226 (1995).

[2] J. E. Segall, S. M. Block, and H. C. Berg, Temporal comparisons in bacterial chemotaxis, Proc. Natl. Acad. Sci. U.S.A. **83**, 8987 (1986).

[3] A. Gosztolai and M. Barahona, Cellular memory enhances bacterial chemotactic navigation in rugged environments, Commun. Phys. **3**, 47 (2020).

[4] D. Lacy and D. P. Christenson, Who votes for the future? Information, expectations, and endogeneity in economic voting, Polit. Behav. **39**, 347 (2017).

[5] M. Fruchart, R. Hanai, P. B. Littlewood, and V. Vitelli, Non-reciprocal phase transitions, Nature (London) **592**, 363 (2021).

[6] S. Galam, Sociophysics: A review of Galam models, Int. J. Mod. Phys. C **19**, 409 (2008).

[7] R. Axelrod, The dissemination of culture–A model with local convergence and global polarization, J. Conflict Resolut. **41**, 203 (1997).

[8] C. Castellano, S. Fortunato, and V. Loreto, Statistical physics of social dynamics, Rev. Mod. Phys. **81**, 591 (2009).

[9] A. Flache, M. Mäs, T. Feliciani, E. Chattoe-Brown, G. Deffuant, S. Huet, and J. Lorenz, Models of social influence: Towards the next frontiers, J. Artif. Soc. Social Simul. **20** 2 (2017).

[10] F. L. Yin, Y. W. She, J. X. Wang, Y. W. Wu, and J. H. Wu, Modeling and analyzing information propagation evolution integrating internal and external influences, Adv. Theory Simul. **7**, 2300845 (2024).

[11] G. W. Breslauer and K. J. Breslauer, Political science meets physical science: The shared concept of stability, PNAS Nexus **2**, pgad401 (2023).

[12] R. Axelrod, J. J. Daymude, and S. Forrest, Preventing extreme polarization of political attitudes, Proc. Natl. Acad. Sci. U.S.A. **118**, e2102139118 (2021).

[13] S. Li, T. V. Phan, G. Wang, R. Khuri, J. W. Wilson, R. H. Austin, and L. Liu, Memory of elastic collisions drives high minority spin and oscillatory entropy in underdamped chiral spinners, Commun. Phys. **7**, 136 (2024).

[14] See Supplemental Material at http://link.aps.org/supplemental/10.1103/rt97-ncmf for experiment details and theory derivation.

[15] H. Yu, Y. Fu, X. Zhang, L. Chen, D. Qi, J. Shi, and W. Wang, Programmable active matter across scales, Programmable Mater. **1**, e7 (2023).

[16] B. VanSaders, M. Fruchart, and V. Vitelli, Measurement-induced phase transitions in informational active matter, PNAS Nexus pgag077 (2026).

[17] J. Chen, X. Lei, Y. Xiang, M. Duan, X. Peng, and H. P. Zhang, Emergent chirality and hyperuniformity in an active mixture with nonreciprocal interactions, Phys. Rev. Lett. **132**, 118301 (2024).

[18] S. Li, B. Dutta, S. Cannon, J. J. Daymude, R. Avinery, E. Aydin, A. W. Richa, D. I. Goldman, and D. Randall, Programming active cohesive granular matter with mechanically induced phase changes, Sci. Adv. **7**, eabe8494 (2021).

[19] S. Galam, Unanimity, coexistence, and rigidity: Three sides of polarization, Entropy **25**, 622 (2023).

[20] C. W. Lynn, L. Papadopoulos, D. D. Lee, and D. S. Bassett, Surges of collective human activity emerge from simple pairwise correlations, Phys. Rev. X **9**, 011022 (2019).

[21] J. L. Silverberg, M. Bierbaum, J. P. Sethna, and I. Cohen, Collective motion of humans in mosh and circle pits at heavy metal concerts, Phys. Rev. Lett. **110**, 228701 (2013).

[22] M. Te Vrugt, J. Bickmann, and R. Wittkowski, Effects of social distancing and isolation on epidemic spreading modeled via dynamical density functional theory, Nat. Commun. **11**, 5576 (2020).

[23] C. Kaspar, B. J. Ravoo, W. G. van der Wiel, S. V. Wegner, and W. H. Pernice, The rise of intelligent matter, Nature (London) **594**, 345 (2021).

[24] M. Brandenbourger, X. Locsin, E. Lerner, and C. Coulais, Non-reciprocal robotic metamaterials, Nat. Commun. **10**, 4608 (2019).

[25] C. Scholz, A. Ldov, T. Pöschel, M. Engel, and H. Löwen, Surfactants and rotelles in active chiral fluids, Sci. Adv. **7**, eabf8998 (2021).

[26] C. Scholz, M. Engel, and T. Pöschel, Rotating robots move collectively and self-organize, Nat. Commun. **9**, 931 (2018).

[27] X. Yang, C. Ren, K. Cheng, and H. P. Zhang, Robust boundary flow in chiral active fluid, Phys. Rev. E **101**, 022603 (2020).

[28] T. H. Tan, A. Mietke, J. Li, Y. Chen, H. Higinbotham, P. J. Foster, S. Gokhale, J. Dunkel, and N. Fakhri, Odd dynamics of living chiral crystals, Nature (London) **607**, 287 (2022).

[29] Y. Zhang, Q. Liu, Z. Wang, and S. Zhang, On the opinion formation of mobile agents with memory, Physica (Amsterdam) **492A**, 438 (2018).

[30] M. Mijalkov, A. McDaniel, J. Wehr, and G. Volpe, Engineering sensorial delay to control phototaxis and emergent collective behaviors, Phys. Rev. X **6**, 011008 (2016).

[31] C. Chen, S. Liu, X.-q. Shi, H. Chaté, and Y. Wu, Weak synchronization and large-scale collective oscillation in dense bacterial suspensions, Nature (London) **542**, 210 (2017).

[32] X. Guo, M. Guzmán, D. Carpentier, D. Bartolo, and C. Coulais, Non-orientable order and non-commutative response in frustrated metamaterials, Nature (London) **618**, 506 (2023).

[33] N. E. Leonard, K. Lipsitz, A. Bizyaeva, A. Franci, and Y. Lelkes, The nonlinear feedback dynamics of asymmetric political polarization, Proc. Natl. Acad. Sci. U.S.A. **118**, e2102149118 (2021).

[34] C. W. Lynn, L. Papadopoulos, A. E. Kahn, and D. S. Bassett, Human information processing in complex networks, Nat. Phys. **16**, 965 (2020).

[35] Y. Jiang, Q. Mi, and L. Zhu, Neurocomputational mechanism of real-time distributed learning on social networks, Nat. Neurosci. **26**, 506 (2023).

[36] G. S. Guralnik, The history of the guralnik, hagen and kibble development of the theory of spontaneous symmetry breaking and gauge particles, Int. J. Mod. Phys. A **24**, 2601 (2009).

[37] L. Xu, D. Patterson, S. A. Levin, and J. Wang, Non-equilibrium early-warning signals for critical transitions in ecological systems, Proc. Natl. Acad. Sci. U.S.A. **120**, e2218663120 (2023).

[38] S. H. Strogatz, *Nonlinear Dynamics and Chaos: With Applications to Physics, Biology, Chemistry, and Engineering* (Westview Press, Boulder, CO, 2015), 3rd ed.

[39] G. Wang, T. V. Phan, S. Li, J. Wang, Y. Peng, G. Chen, J. Qu, D. I. Goldman, S. A. Levin, K. Pienta *et al.*, Robots as models of evolving systems, Proc. Natl. Acad. Sci. U.S.A. **119**, e2120019119 (2022).

[40] C. O. Barkan and S. Wang, Multiple phase transitions shape biodiversity of a migrating population, Phys. Rev. E **107**, 034405 (2023).

[41] C. E. Shannon, A mathematical theory of communication, Bell Syst. Tech. J. **27**, 379 (1948).

[42] B. Chong, J. He, D. Soto, T. Wang, D. Irvine, G. Blekherman, and D. I. Goldman, Multilegged matter transport: A framework for locomotion on noisy landscapes, Science **380**, 509 (2023).

[43] S. Galam, Fake news: "No ban, no spread—With sequestration," Physics **6**, 859 (2024).

[44] M. E. Cates and C. Nardini, Classical nucleation theory for active fluid phase separation, Phys. Rev. Lett. **130**, 098203 (2023).

[45] S. Galam, Contrarian deterministic effects on opinion dynamics: "The hung elections scenario," Physica (Amsterdam) **333A**, 453 (2004).

[46] C. Yan, D. Guan, Y. Wang, P.-Y. Lai, H.-Y. Chen, and P. Tong, Avalanches and extreme value statistics of a mesoscale moving contact line, Phys. Rev. Lett. **132**, 084003 (2024).

[47] M. Fruchart, R. Hanai, P. B. Littlewood, and V. Vitelli, Non-reciprocal phase transitions, Nature (London) **592**, 363 (2021).

[48] H. Ebbinghaus, *Über das Gedächtnis: Untersuchungen zur Experimentellen Psychologie* (Duncker & Humblot, Leipzig, 1885).

[49] D. C. Rubin, S. Hinton, and A. Wenzel, The precise time course of retention, J. Exp. Psychol. Learn. Memory Cognit. **25**, 1161 (1999).

[50] P. Woźniak, E. Gorzelańczyk, and J. Murakowski, Two components of long-term memory, Acta Neurobiol. Exp. **55**, 301 (1995).

[51] L. B. Solum, Originalism versus living constitutionalism: The conceptual structure of the great debate, Northwest. Univ. Law Rev. **113**, 1243 (2018).

[52] M. Z. Miskin, A. J. Cortese, K. Dorsey, E. P. Esposito, M. F. Reynolds, Q. Liu, M. Cao, D. A. Muller, P. L. McEuen, and I. Cohen, Electronically integrated, mass-manufactured, microscopic robots, Nature (London) **584**, 557 (2020).

[53] M. M. Lassiter, J. Lee, K. Skelil, L. Xu, L. Hanson, W. H. Reinhardt, D. Sylvester, M. Yim, D. Blaauw, and M. Z. Miskin, Microscopic robots that sense, think, act, and compute, Sci. Robot. **10**, eadu8009 (2025).

[54] S. Li, Data for "Informational Memory Shapes Collective Behavior in Intelligent Swarms" (2026), 10.5281/zenodo.13761531.